HHS Public Access

Author manuscript

Sci Transl Med. Author manuscript; available in PMC 2017 December 27.

Published in final edited form as:

Sci Transl Med. 2017 June 28; 9(396): . doi:10.1126/scitranslmed.aal4649.

Linker proteins restore basement membrane and correct *LAMA2*-related muscular dystrophy in mice

Judith R. Reinhard[1], **Shuo Lin**[1], **Karen K. McKee**[2], **Sarina Meinen**[1], **Stephanie C. Crosson**[2], **Maurizio Sury**[1], **Samantha Hobbs**[2], **Geraldine Maier**[1], **Peter D. Yurchenco**[2], and **Markus A. Rüegg**[1,*]

[1]Biozentrum, University of Basel, 4056 Basel, Switzerland [2]Robert Wood Johnson Medical School, Rutgers University, Piscataway, NJ 08854, USA

Abstract

LAMA2-related muscular dystrophy (*LAMA2* MD or MDC1A) is the most frequent form of early-onset, fatal congenital muscular dystrophies. It is caused by mutations in *LAMA2*, the gene encoding laminin-α2, the long arm of the heterotrimeric (α2, β1, and γ1) basement membrane protein laminin-211 (Lm-211). We establish that despite compensatory expression of laminin-α4, giving rise to Lm-411 (α4, β1, and γ1), muscle basement membrane is labile in *LAMA2* MD biopsies. Consistent with this deficit, recombinant Lm-411 polymerized and bound to cultured myotubes only weakly. Polymerization and cell binding of Lm-411 were enhanced by addition of two specifically designed linker proteins. One, called αLNNd, consists of the N-terminal part of laminin-α1 and the laminin-binding site of nidogen-1. The second, called mini-agrin (mag), contains binding sites for laminins and α-dystroglycan. Transgenic expression of mag and αLNNd in a mouse model for *LAMA2* MD fully restored basement membrane stability, recovered muscle force and size, increased overall body weight, and extended life span more than five times to a maximum survival beyond 2 years. These findings provide a mechanistic understanding of *LAMA2* MD and establish a strong basis for a potential treatment.

INTRODUCTION

Skeletal muscle is the largest organ in the human body accounting for up to 50% of its mass. The functional units of skeletal muscle are singly innervated muscle fibers that are formed by the fusion of myoblasts to multinucleated cells. To withstand the mechanical force generated during contraction, muscle fibers are surrounded by basement membrane (BM), a

*Corresponding author. markus-a.ruegg@unibas.ch.

Author contributions: J.R.R., P.D.Y., and M.A.R. designed experiments. J.R.R., S.L., S.M., S.C.C., M.S., and G.M. performed experiments and analyzed the data. K.K.M., with the help of S.H., generated and characterized antibodies and recombinant laminins and provided all the data shown in Fig. 2. J.R.R. and M.A.R. wrote the manuscript.

Competing interests: All authors declare that they have no competing interests.

Data and materials availability: Relevant data that support the findings of this study are available from M.A.R. (markus-a.ruegg@unibas.ch) upon request.

highly structured assembly of extracellular matrix proteins. The bond between the muscle plasma membrane (called sarcolemma) and BM is crucial for muscle fiber stability and signal transduction. Mutations in BM proteins, their receptors, or cytosolic adaptors can cause muscular dystrophies of different severity and time of onset (1).

Congenital muscular dystrophy (CMD) is a group of muscular dystrophies characterized by an early onset. *LAMA2*-related muscular dystrophy (*LAMA2* MD), also called muscular dystrophy congenital type 1A (MDC1A or merosin-deficient CMD), is among the most frequent CMDs in Europe (2, 3). It is caused by mutations in the *LAMA2* gene encoding the α2 subunit of laminin-211 (Lm-211). Most *LAMA2* MD patients show complete absence of laminin-α2, are hypotonic (floppy) at birth, fail to ambulate, and succumb to respiratory complication. Patients with less severe symptoms often express low amounts of laminin-α2 or a truncated form (4). Several mouse models for *LAMA2* MD exist (5). Most widely used are the dy^W/dy^W mice (6) that show a very early-onset muscular dystrophy and a markedly shortened life span. A less severe model, dy^{2J}/dy^{2J} mice, expresses an N-terminally truncated mutant of laminin-α2 and shows a mild dystrophic pathology (7, 8).

Lm-211, a heterotrimer of the α2, β1, and γ1 chains, is the prevalent laminin found in both the endomysial BM of mature skeletal muscle and the Schwann cells of peripheral nerves (9). During embryonic development, muscle BM is composed of Lm-411 (α4, β1, and γ1), Lm-511 (α5, β1, and γ1), and Lm-211 (10). In rodent muscle, laminin-α4 and laminin-α5 disappear postnatally from the BM except at the neuromuscular junctions, with laminin-α2 becoming the major subunit in adults (9). In *LAMA2* MD mouse models, laminin-α4 expression remains elevated into adulthood (9, 11, 12). Laminin-α4 lacks the laminin N-terminal (LN) globule. In vitro BM assembly assays in combination with mutational analysis of Lm-111 (α1, β1, and γ1) suggested that LN globules are important for Lm-111 self-polymerization (13, 14). Moreover, the C-terminal laminin globular (LG) domains of laminin-α4 bind only weakly to the laminin-α2 receptors α-dystroglycan (αDG) and $\alpha_7\beta_1$ integrin (15–17).

We have previously demonstrated that transgenic expression of a miniaturized form of the protein agrin, called mini-agrin (mag), can substantially ameliorate muscular dystrophy in *LAMA2* MD mice (12, 18). This function is based on the binding of mag to the coiled-coil domain of laminins at one end and to αDG at the other, thereby improving BM stability (19). Although this strategy confers strong benefits, muscular dystrophy still progresses in mag-expressing mice and life expectancy remains markedly shorter than in wild-type controls (12, 19). Here, we tested whether additional restoration of laminin's polymerization activity could further improve muscle structure and function in severely dystrophic dy^W/dy^W mice by introducing an additional fusion protein, called αLNNd (laminin-α1 LN-domain nidogen-1) (20). Recent work showed that expression of αLNNd substantially ameliorates disease in dy^{2J}/dy^{2J} mice (21). We now establish that combined expression of αLNNd and mag in dy^W/dy^W mice fully restores muscle BM and extends maximum survival beyond 2 years. These data demonstrate that defects in BM assembly and its proper connection to the sarcolemma are the primary cause of *LAMA2* MD. The use of mag and αLNNd may open new possibilities to treat *LAMA2* MD.

RESULTS

Muscle BM is deficient in *LAMA2* MD patients

Lama2-deficient mice show prominent increases in laminin-α4 and, to a lesser extent, laminin-α5 expression (9, 11, 12, 18). To examine laminin expression in human patients, we stained muscle biopsies from muscular dystrophy patients, selected to be negative for any laminin-α2–like immunoreactivity (fig. S1A), with antibodies against laminin-α4. We observed strong laminin-α4 immunoreactivity colocalizing with laminin-β1γ1 in *LAMA2* MD patients (Fig. 1A). In biopsies of age-matched controls, laminin-α4 immunoreactivity was either very low or not detected in muscle BM (Fig. 1A), except at the neuromuscular junction and in blood vessel BM (fig. S1B). Western blot analysis revealed an increase in laminin-α4 as compared to controls (Fig. 1B). Because the amount of laminin-β1γ1 was not different between *LAMA2* MD patients and controls (Fig. 1B), the loss of laminin-α2 seems compensated for by the increase in laminin-α4. In dy^W/dy^W mice (6), the distribution of laminin-α4 in 8-week-old triceps muscle was very similar to that observed in human biopsies (Fig. 1C). Laminin-α4 expression, as measured by Western blot analysis, was higher than in wild-type mice, whereas laminin-β1γ1 expression was unchanged (Fig. 1D). Transcriptional changes in *Lama4* coincided with increased laminin-α4 in dy^W/dy^W muscle (Fig. 1D). Both wild-type and dy^W/dy^W mice expressed a similar amount of laminin-α4 at birth (fig. S2, A and B). Although expression of laminin-α4 decreased over the next 8 weeks in wild-type mice, it remained high in dy^W/dy^W mice (fig. S2B), suggesting that dy^W/dy^W mice continue to express the embryonic laminin-α4, whereas this isoform is progressively replaced by laminin-α2 in wild-type mice. We also observed a similar increase, although less strong than laminin-α4, of laminin-α5 in both *LAMA2* MD patients and dy^W/dy^W mice (fig. S3). In summary, these results show that expression of the embryonic laminin-α4 and laminin-α5 isoforms remains high in muscle BM in both *LAMA2* MD patients and dy^W/dy^W mice, without alterations in either laminin-β1 or laminin-γ1 expression. These results confirm previous immunostainings of biopsies from *LAMA2* MD patients (22, 23) and support the notion that dy^W/dy^W mice closely resemble the human disease.

To investigate why Lm-411 cannot functionally compensate for the loss of Lm-211, muscle BM in *LAMA2* MD biopsies was analyzed by subcellular fractionation using a combination of differential extraction, enzymatic digestion, and ultracentrifugation (Fig. 1E). Similar methods have been used to determine BM stability in dy^{2J}/dy^{2J} mice, the mouse model expressinga truncated form of laminin-α2 (8). After removal of soluble and membrane proteins, the second pellet (P2) was treated with collagenase to release loosely attached BM proteins into the third supernatant (S3) (Fig. 1E). Finally, stably bound components of the BM from P3 were solubilized by adding high concentrations of EDTA and appeared in S4. Incontrol biopsies, soluble proteins were enriched in S1, membrane proteins were enriched in S2, and laminin-β1γ1 appeared in S4 (Fig. 1F). Analysis of S3 and S4 fractions from control patients showed that laminin-α2 predominately appeared in S4 (Fig. 1G, left lanes, top). Laminin-α4, however, was recovered from fraction S3 in *LAMA2* MD patient samples (Fig. 1G, right lanes, middle). To compare the distribution of all laminin isoforms in S3 and S4, we also probed for laminin-β1γ1 in controls and *LAMA2* MD patients. Laminin-β1γ1 appeared predominately in S4 for controls but was mainly detected in S3 for *LAMA2* MD

patients (Fig. 1G, bottom and right). These results show that Lm-211 is strongly attached to the BM in controls, whereas the compensatory Lm-411 in *LAMA2* MD patients is weakly attached.

αLNNd and mag induce accumulation of Lm-411 on C2C12 myotubes

Reasons for the weak BM attachment of Lm-411 could be lack of the LN globule, which is important for Lm-111 self-polymerization in vitro (24), or lack of binding to αDG and $\alpha_7\beta_1$ integrin, as observed in binding assays using laminin-α4 fragments (Fig. 2A) (15–17). In previous work, we showed that mag binds to laminins via high-affinity binding to the coiled-coil domain (25, 26) and to αDG (27) (Fig. 2A and fig. S4A) but is unlikely to bind to $\alpha_7\beta_1$ integrins (28). Other work has shown that a chimeric protein, called αLNNd, restores polymerization of LN-truncated Lm-111 (ΔLN–Lm-111) and improves binding of ΔLN–Lm-111 to cultured Schwann cells (20). αLNNd comprises the LN domain of laminin-α1 and the laminin/collagen IV binding site of nidogen-1 (Fig. 2A and fig. S4B). Because previous experiments used only fragments of Lm-411 to measure binding affinities to $\alpha_7\beta_1$ integrins and to αDG, we compared binding of recombinant, full-length Lm-411 and Lm-111. In contrast to the Lm-111 control, no or very little binding of Lm-411 to integrin $\alpha_7X_2\beta_1$ (Fig. 2B) or to αDG (Fig. 2C) was detected. Adding an equimolar concentration of purified mag increased binding of Lm-411 to αDG (Fig. 2D). Mag also significantly improved binding of recombinant, full-length Lm-511 to αDG (fig. S4C). Self-polymerization of recombinant Lm-411 was measured using a sedimentation technique previously used with truncated Lm-111 (20). Whereas Lm-111 polymerized with increasing concentrations, Lm-411 did not polymerize (Fig. 2E). Lm-411 combined with equimolar concentrations of αLNNd, however, dose-dependently formed polymers similar to Lm-111 (Fig. 2E).

Finally, we assessed the ability of mag and αLNNd to promote binding of Lm-411 to cultured C2C12 myotubes grown to confluence. In contrast to Lm-211, Lm-411 did not bind to C2C12 myotubes (Fig. 2F). Whereas an equimolar concentration of mag improved binding, no significant increase was observed in the presence of αLNNd alone (Fig. 2F). Combined addition of mag and αLNNd, however, enhanced binding of Lm-411, reaching a similar staining intensity as for Lm-211 (Fig. 2F). These experiments suggest that αLNNd promotes Lm-411 polymerization, whereas mag mediates high-affinity binding to αDG, and together, they may be sufficient to compensate for the loss of Lm-211 in *LAMA2* MD.

Muscle BMs are fully restored in double-transgenic dy^W/dy^W mice

To test this hypothesis, we generated double-transgenic dy^W/dy^W mice that expressed αLNNd and mag. To allow comparison with previous work using mag (12, 18, 19, 29), expression of αLNNd was driven by the same muscle creatine kinase (MCK) promoter. Two stable αLNNd transgenic mouse lines were established, which were independently mated to obtain mice of the following genotypes: dy^W/dy^W mice, dy^W/dy^W mice expressing mag (dy^W/dy^W mag), dy^W/dy^W mice expressing αLNNd (dy^W/dy^W αLNNd), and dy^W/dy^W mice expressing both transgenes (dy^W/dy^W DT). Western blot analysis of total lysates from 8-week-old triceps muscle demonstrated the presence of the transgenes (Fig. 3A). The two independent dy^W/dy^W αLNNd lines A and B expressed similar amounts of the transgene

(fig. S5A). Because there was also no difference in the phenotypes between dy^W/dy^W DT mice of each line (fig. S5, B and C), we focused our analysis on line A. Both the mag and the αLNNd transgenic proteins were already present at birth (P0), and their amount seemed to increase over the first three postnatal weeks (fig. S5, D and E). As noted previously (12), the mag transgene appeared on Western blots as two bands with an apparent M_r (relative molecular mass) of 80 and 110 kDa, respectively (Fig. 3A and fig. S5E). The upper band corresponds to the full-length mag protein, whereas the lower band is the result of proteolytic cleavage by the agrin-specific protease neurotrypsin (30), as shown by immunoprecipitation/SDS-PAGE followed by tandem mass spectrometry (fig. S5F) and mag expression in neurotrypsin-deficient mice (fig. S5G). At 8 weeks of age, αLNNd and mag proteins colocalized perfectly with laminin-g1 in dy^W/dy^W DT mice, indicating that both transgenes were incorporated into the muscle BM (Fig. 3B). Both transgenic proteins were bound to Lm-411, as shown by coimmunoprecipitation (Fig. 3C). The expression of the transgenes did not affect the total amount of laminin-α4 or of laminin-$\beta_1\gamma_1$ (Fig. 3, D and E) compared to nontransgenic dy^W/dy^W mice.

To test whether the transgenes changed attachment of laminin-α4 to muscle BM, differential extraction was used (Fig. 1E). In dy^W/dy^W mice, most laminin-α4 appeared in fraction S1, which contains secreted and cytosolic proteins. The majority of the remaining laminin-α4 was recovered in S3, and only a minor fraction appeared in S4 (Fig. 4A). Whereas mag did not change the distribution of laminin-α4 in the different fractions, αLNNd increased the proportion in S4 (Fig. 4A). In dy^W/dy^W DT mice, the proportion of laminin-α4 was reduced in S1 but increased in S4 compared to dy^W/dy^W mice, demonstrating a striking improvement of laminin-α4 incorporation into BM (Fig. 4A). To examine the association of all laminin isoforms with the BM, we compared the proportion of laminin-β1γ1 present in each fraction (Fig. 4B). The proportion of laminin-β1γ1 in the S4 fraction of single transgenic mice (dy^W/dy^W mag or dy^W/dy^WαLNNd) was improved compared to dy^W/dy^W mice but was still lower than that in wild-type mice. In contrast, the proportion of laminin-β1γ1 in the S4 fraction of dy^W/dy^W DT mice was indistinguishable from that seen in wild-type mice and higher than either single transgenic mouse (Fig. 4B). Furthermore, in dy^W/dy^W DT mice, the amount of mag and αLNNd was higher in the S4 fraction relative to the S3 fraction (fig. S5H), showing cofractionation of the transgenic proteins with Lm-411. Finally, BM structure, judged by electron density and continuity, was indistinguishable between dy^W/dy^W DT mice and wild-type littermate controls (Fig. 4C). In contrast, BMs in dy^W/dy^W mice appeared patchy and of low electron density (Fig. 4C), whereas single transgenic mice showed an intermediate improvement in BM structure (Fig. 4C). These results demonstrate that simultaneous expression of mag and αLNNd in dy^W/dy^W mice mediates incorporation of Lm-411 into the BM and restores BM structure to an extent that reaches the quality of wild-type controls.

Transgenes greatly ameliorate muscular dystrophy

To test whether the restoration in BM structure also improved function, we next examined histology of skeletal muscle by staining cross sections with hematoxylin and eosin (H&E). Triceps from 8-week-old dy^W/dy^W mice showed signs of muscular dystrophy, including fibrotic regions, centralized myonuclei indicating muscle fiber degeneration/regeneration,

and differences in fiber size (Fig. 5A). Expression of a single transgene improved but did not completely overcome these pathological indicators, whereas dy^W/dy^W DT histology was comparable to wild-type controls with the exception of centralized myonuclei (Fig. 5A). Qualitative assessment of fibrosis by collagen staining with Sirius Red dye also showed that the transgenes reduced fibrosis (Fig. 5B). The collagen content, as quantified by the relative amount of hydroxyproline, was reduced to amounts similar to those in wild-type mice (Fig. 5C). Quantitative assessment of histological changes, such as fiber size variation, median fiber size, and total fiber number, revealed that the single transgenes ameliorated the muscular dystrophy and that the double-transgenic dy^W/dy^W DT mice reached values similar to those of wild-type controls (Fig. 5D and table S1). Fibrosis in dy^W/dy^W correlated with increased inflammation (macrophages stained with anti-F4/80 antibodies) in cross sections of 8-week-old triceps muscle (fig. S6) and an almost 10-fold increase in the F4/80-encoding transcript *Adgre1* (Fig. 5E). Macrophage number and levels of *Adgre1* were decreased by the transgenes (fig. S6 and Fig. 5E). A very similar normalization by the transgenes was observed for *Tnc* expression, encoding the matricellular protein tenascin-C, shown to be increased in dy^W/dy^W mice (31, 32).

Quantification of the percentage of muscle fibers with centralized myonuclei (CNFs) indicated that single- and double-transgenic dy^W/dy^W mice had the same or an even higher number of such fibers (Fig. 5G). Centralized myonuclei in muscular dystrophies are indicative of recent muscle regeneration as the consequence of previous muscle degeneration. Although the number of centralized myonuclei in dy^W/dy^W mice is increased, there is also evidence that regenerating fibers undergo apoptosis (29, 33, 34), thus hampering successful regeneration and lowering the number of centralized myonuclei. Consequently, treatments that improve survival of regenerating fibers, such as expression of Bcl2, result in a higher number of fibers with centralized myonuclei (29). On the other hand, treatments that prevent muscle degeneration will lower the percentage of muscle fibers with centralized myonuclei. In previous work, we have shown that mag both lowers muscle degeneration and improves muscle regeneration (19). This dual function results in an increased number of fibers with centralized myonuclei in dy^W/dy^W mag mice compared to dy^W/dy^W mice (29), which is consistent with our data in 8-week-old mice (Fig. 5G). To explore possible reasons for the high number of centralized myonuclei in dy^W/dy^W DT mice, we examined cross sections of triceps muscle from 3-week-old mice using H&E (fig. S7A) and Sirius Red staining (fig. S7B). At this early time point, the triceps of dy^W/dy^W DT mice showed similar signs of muscular dystrophy as did those of dy^W/dy^W mice (fig. S7, A and B). In addition, analysis of 3-week-old muscle for the presence of the embryonic form of myosin heavy chain (eMHC) indicated that dy^W/dy^W DT mice show a high degree of regeneration (fig. S7, C and D). At the age of 8 weeks, dy^W/dy^W DT mice contained only few eMHC-positive fibers compared to dy^W/dy^W mice (fig. S7E), and the amount of eMHC detected in lysates was not different from that in wild-type controls (fig. S7F). These data suggest that because of the low expression of mag and αLNNd in the first postnatal weeks (fig. S5, D and E), stabilization of muscle BM might only be achieved later, leaving the myonuclei still at a central position at 8 weeks of age. Consistent with this idea, the number of fibers with centralized myonuclei in the triceps of dy^W/dy^W DT mice was significantly higher at 3 weeks than at 8 weeks (fig. S7G).

Expression of the transgenes had a very similar ameliorating effect in 8-week-old tibialis anterior (TA) muscle (fig. S8, A and B) and the diaphragm (fig. S8C) as in triceps muscle. Quantification of fibrosis by either measuring hydroxyproline content (Fig. 5H for TA) or determining the Sirius Red–positive area (Fig. 5I for diaphragm) confirmed the substantial improvement by single transgenes and the reduction close to wild-type by the simultaneous action of both transgenes. Finally, we measured creatine kinase activity in the blood as an estimate for damage of all skeletal muscles. Again, dy^W/dy^W DT mice were improved compared to dy^W/dy^W and not different from wild-type controls (Fig. 5J).

Next, we assessed disease progression in 16-week-old mice. We excluded dy^W/dy^W mice in this analysis because of their low survival rate. Gross muscle architecture and fibrosis remained markedly improved in the double-transgenic compared to single-transgenic dy^W/dy^W mice, as quantified by the variance coefficient of fiber diameter (fig. S9A) and the relative content of hydroxyproline in triceps (fig. S9B) and TA (fig. S9C). In summary, the overall histological phenotype of dy^W/dy^W DT muscle became similar to that in wild-type mice, with the notable exception that the number of centralized myonuclei was higher than that in wild-type controls.

Transgenes improve muscle function and markedly prolong life span

At the age of 8 weeks, dy^W/dy^W mice were easily distinguishable from control littermates by their small size and kyphosis (Fig. 6A). dy^W/dy^W DT mice looked similar to control littermates, with the exception of a waddling gait, slight hindlimb paralysis, and a leaner appearance (Fig. 6A). Peripheral neuropathy is a characteristic feature of dy^W/dy^W mice (35), and expression of the transgenes using the MCK promoter does not restore this deficit. Despite this neuropathy, in a vertical grid hang test, dy^W/dy^W DT passed the 3-min test, whereas dy^W/dy^W were largely unable to hold themselves on the grid (Fig. 6B). The expression of mag alone improved hang time, whereas little effect was seen in mice expressing αLNNd (Fig. 6B). Consistent with the improved hang time, peak tetanic force measured in isolated extensor digitorum longus (EDL) at 8 weeks was improved in single- and double-transgenic compared to dy^W/dy^W mice (Fig. 6C). At 16 weeks of age, the effect of the combined expression of mag and αLNNd was superior to mice expressing only one transgene (Fig. 6D). Similar results were obtained for the peak twitch force and measurements in soleus muscles (table S2). Notably, these improvements in force were evident in spite of the muscle atrophy resulting from hindlimb paralysis.

To further assess the therapeutic potential of combined mag and αLNNd expression, we measured body mass and life span. Both body mass and life span were drastically reduced in dy^W/dy^W mice, with a peak body mass of about 9 g and a median survival of just 15.5 weeks. The expression of mag or αLNNd resulted in an about 40% increase in body mass and in extended life span. Median life span reached 50 weeks in dy^W/dy^W mag mice, as reported before (19). The survival curve of dy^W/dy^W αLNNd mice was biphasic, extending the survival of long survivors (9 of 16) only. The expression of both transgenes together increased body mass by more than 90% and increased life span, with a median life span of 81 weeks and 5 of 16 mice reaching an age beyond 2 years. Two-year-old dy^W/dy^W DT mice were quite active in spite of the complete hindlimb paralysis (fig. S10A). Examination

of muscle histology in the triceps and the diaphragm showed preservation of muscle tissue (fig. S10, B and C). Finally, staining triceps muscles of the 2-year-old mice for laminin-α4 and laminin-α5 showed that the sarcolemmal BM of dy^W/dy^W DT mice still contained high amounts of both proteins, whereas the two laminin-a chains were confined to blood vessels in wild-type controls (fig. S10, D and E). In summary, these data show that expression of a single transgene leads to a modest increase in body mass and a robust extension of life span. Combined expression of mag and αLNNd has an even more profound effect that includes stabilization of body weight and prolonged preservation of muscle histology, which together allows some of these transgenic mice to survive as long as control littermates in spite of the complete hindlimb paralysis.

DISCUSSION

Our work provides a framework for the mechanistic understanding of *LAMA2* MD and presents an efficacious preclinical treatment. The approach is based on the observation that muscle BM of *LAMA2* MD patients is unstable despite the compensatory increase of laminin-α4. This phenomenon was also observed in dy^W/dy^W mice. Thus, the disease pathology in dy^W/dy^W mice mirrors that seen in *LAMA2* MD patients not only phenotypically but also mechanistically. Wild-type and dy^W/dy^W mice express high levels of laminin-α4 at birth. Whereas laminin-α2 replaces laminin-α4 in muscle BM postnatally in wild-type mice, laminin-α4 remains high throughout the life span of dy^W/dy^W mice. Such sustained expression of laminin-α4 is a unique feature of *LAMA2* MD. The slight increase of laminin-α5 in *LAMA2* MD patients and mouse models, in contrast, may be the consequence of ongoing muscle degeneration/regeneration, because such increase has been observed during muscle regeneration after injury (36) and in several other muscular dystrophies (37). Laminin-α4 and laminin-α5 persist in the muscle BM of *LAMA2* MD patients at an age of at least 14 years (the oldest donor in our cohort), suggesting that the therapeutic translation of this approach into clinics should be possible well after the onset of the disease.

The therapeutic approach presented here uses the specific increase of laminin-α4 in *LAMA2* MD as the binding scaffold for the two linker proteins, mag and αLNNd. A cornerstone of this study was our finding that combined expression of mag and αLNNd is sufficient to enhance the cell binding and polymerization capacity of Lm-411 in cultured C2C12 myotubes. These findings were corroborated in vivo, with the combination of mag and αLNNd restoring BM structure and function in dystrophic dy^W/dy^W mice. In contrast, expression of either transgene singly only partially shifted extractability of Lm-411 and partially improved BM structure. These results are thus the direct in vivo support for the model (14) that the formation and maintenance of the primary laminin network require both cell surface binding (restored in the dy^W/dy^W DT mice by mag) and laminin self-assembly (restored by αLNNd). The therapeutic effect of a single transgene in dy^W/dy^W mice may be based on the increased amount of laminin-α5. In the dy^W/dy^W mag mice, Lm-511 could provide the necessary LN domains to form laminin hetero-oligomers with Lm-411, whereas binding to muscle fibers would be mediated by mag (12). Similar hetero-oligomers between Lm-411 and Lm-511 could also be formed in dy^W/dy^WαLNNd, with the laminin-α5 mediating some binding to muscle receptors. The laminin self-assembly model (14) is also

supported by the finding that transgenic expression of αLNNd alone is sufficient to ameliorate muscle function and BM structure in dy^{2J}/dy^{2J} mice (21). Muscular dystrophy in dy^{2J}/dy^{2J} mice is due to an N-terminal truncation of laminin-α2, representing a mild form of *LAMA2* MD. In these mice, laminin-α2 still contains all the C-terminal LG domains that bind to the sarcolemma, and thus, restoration of laminin self-assembly by αLNNd is sufficient [see also commentary (38)].

Lack of Lm-211 causes structural instability to contracting muscle fibers, leading to their degeneration. This then initiates a cascade of secondary events, which all accelerate disease progression. The secondary events, such as apoptosis/necrosis of regenerating muscle fibers, inflammation, and fibrosis, are often common to several muscular dystrophies (39). Although approaches to inhibit such downstream events are applicable to several diseases, their efficacy is limited. For example, inhibition of fibrosis by the angiotensin II type 1 receptor blocker losartan ameliorates the disease in mouse models for Marfan's syndrome, Duchenne muscular dystrophy, and *LAMA2* MD (40–42). In dy^{W}/dy^{W} mice, losartan treatment dampens the expression of matricellular proteins, a class of matrix proteins that does not contribute directly to BM structure but rather serves as regulators of cell function (43). Increased expression of matricellular proteins is an early disease marker in dy^{W}/dy^{W} mice (32), and there is evidence that normalization of those markers, in conjunction with the improvement of muscle regeneration, ameliorates disease progression (44). We examined the expression of the matricellular protein tenascin-C and found that its expression was the same as that in wild-type controls upon expression of both linker proteins. Together with our data demonstrating reduction of fibrosis and inflammation, these data indicate that prevention of the primary deficit of muscle BM instability in *LAMA2* MD prevents secondary events.

Forced expression of *Lama1*, encoding laminin-α1, also tackles the structural deficit in *LAMA2* MD. In these experiments, ubiquitous transgenic expression fully restored the functionality of the BM and prolonged survival of dystrophic mice for up to 2 years (45, 46). Because the transgene was also expressed in the peripheral nerve, the mice did not show hindlimb paralysis. Although this is proof that laminin-α1 can replace laminin-α2, translation of this approach into clinics is fraught with challenges. *LAMA1* is too large to insert into suitable gene therapy vectors; production of Lm-111, with a size of about 850 kDa, is challenging; and the efficacy of injected protein remains low (47, 48). The strategy presented here, in contrast, has potential for translation into clinics because the complementary DNAs (cDNAs) encoding αLNNd or mag are small and can be incorporated into adeno-associated virus (AAV) vectors. First, systemic application of muscle-targeted AAV that expresses mag ameliorated the disease phenotype in dy^{W}/dy^{W} mice to a similar extent as transgenic expression (49). Second, AAV-mediated gene transfer into skeletal muscle allows expression of the gene of interest for at least 10 years in human patients (50). Third, both linker proteins are secreted and can also be incorporated into the BM in adjacent, noninfected muscle fibers. Fourth, mag and αLNNd are derived from proteins (agrin, laminin-α1, and nidogen-1) that are expressed in *LAMA2* MD patients. Thus, possible immune responses to the expressed linker proteins might be restricted to neoepitopes generated by the fusion of domains from different proteins. Infection efficacy and immune responses are likely less of a challenge than in gene transfer strategies for Duchenne muscular dystrophy, where the transferred microdystrophin can only act in the infected

muscle fibers and patients may generate antibodies against the expressed protein (51). Despite these advantages of our approach, successful translation into patients will require the targeting of all muscles by systemic delivery of AAV. Restoration of whole-body muscle function for at least 9 months has recently been achieved in dog models for X-linked myotubular myopathy by one-time peripheral venous infusion of myotubularin-expressing AAV (52). However, systemic delivery of AAV has not been reported for muscular dystrophy patients. Moreover, high-efficacy treatment of *LAMA2* MD patients would require delivery of two different AAV vectors and at young age. Injection of recombinant proteins might be another option for treatment, but success might be hampered because mag and αLNNd strongly bind to extracellular matrix proteins that are not specific for muscle BM.

On the basis of the data obtained in mice, the combined treatment with mag and αLNNd should greatly improve quality of life measures, such as muscle function and body mass, and most importantly prolong life span. In the mice, median survival increased from 16 weeks for the dy^W/dy^W mice to more than 81 weeks in the dy^W/dy^W DT mice. In the dy^W/dy^W DT mice cohort, one-third of the mice reached an age of more than 2 years, an age that only one-half of female and two-thirds of male wild-type C57/BL6 mice reach (53). The life span extension was achieved despite hindlimb paralysis resulting from defective peripheral nerve myelination, which is not corrected in the transgenic mice due to the muscle-specific expression of the transgenes. The observation that life span extension is possible in spite of hindlimb paralysis also shows that the lower efficacy of the single transgenes is likely based on an incomplete restoration of muscle function and not on phenotypes caused in nonmuscle tissue. Whereas the peripheral neuropathy is a prominent feature of all mouse models of *LAMA2* MD (5), the muscular dystrophy is the predominant phenotype in human patients (54). There is only one case report in which mutations in *LAMA2* have been shown to result in a limb-girdle type of muscular dystrophy with prevalent peripheral nerve involvement (55).

MATERIALS AND METHODS

Study design

The objective of this study was to test the use of two designed small linker proteins for the potential treatment of *LAMA2* MD. We reasoned that addition of these proteins could restore the muscle BM despite Lm-211 deficiency. We tested the capacity of the linker proteins in vitro and by transgenic expression in a mouse model for *LAMA2* MD. No statistical methods were used to predetermine sample sizes, but sample sizes are similar to those reported in the field. We did not use any method of randomization and did not exclude mice from the study except those that died before the planned age of analysis. Evaluations of immunohistochemistry and muscle histology were performed by investigators blinded to the specific sample.

Mice

dy^W/dy^W mice [B6.129S1(Cg)-*Lama2*^{tm1Eeng}/J; available from the Jackson Laboratory] containing a LacZ insertion in the *Lama2* (6) served as mouse model for *LAMA2* MD. Mice

expressing the mag transgene under the MCK promoter were described previously (12). The αLNNd transgene is a chimeric protein consisting of the laminin-α1 LN-LEa domains fused to the C-terminal part of nidogen-1 (G2-G3 domain) (20). Its corresponding cDNA was subcloned into a vector containing the MCK promoter sequence (12). This construct was linearized with Pac I and injected into the pronuclei of fertilized mouse oocytes. We used two lines that expressed αLNNd at high levels. Neurotrypsin-deficient mice were described previously (30). Genotyping of dy^W/dy^W and mag was performed as described previously (6, 12, 19). Genotyping of αLNNd was performed with the following primers: 5′-CTCATCT-CAGAAGAGGATCTG-3′ and 5′-GAATAATACGAGGTGCAGAT-GACTTC-3′. The transgenic mouse lines were maintained on a C57BL/6J background. All mice analyzed were from breedings of $dy^W/+$ mice that were hemizygous for αLNNd or mag, which allowed to receive all genotypes from the same breeding. Control mice were wild type or $dy^W/+$ from the same litters. Unless otherwise indicated, female and male mice were used. To ensure optimal access of the dystrophic mice to water and food, all cages were supplied with long-necked water bottles and wet food. All mouse experiments were performed according to the federal guidelines for animal experimentation and approved by the authorities of the Canton of Basel-Stadt.

Human samples

Muscle biopsies analyzed were from donors of both genders (ages 5 to 16 years). They were collected as extra tissue that was removed during a diagnostic biopsy or as remaining or extra tissue that was removed during a medical procedure after patient consent. Biopsies were received from the Institute of Pathology, University Hospital, Basel, Switzerland, and three institutes associated with EuroBioBank (www.eurobiobank.org) and TREAT-NMD (www.treat-nmd.eu): the “Myobank AFM” hosted by the Institute de Myologie, Paris, France; the “Cells, tissues and DNA from patients with neuromuscular diseases” hosted by C. Besta Neurological Institute, Milano, Italy (funded by the Telethon Network of Genetic Biobanks, project no. GTB12001); and “The Muscle Tissue Culture Collection” hosted by the Friedrich-Baur-Institute, Munich, Germany [associated with MD-NET and mito-NET, which are both funded by Federal Ministry of Education and Research (BMBF)].

Antibodies

For immunostaining and Western blot analysis, the following antibodies were used: α-actinin (1:5000; Sigma, catalog no. A7732), agrin [chicken, for detection of mag, produced in-house (56), 1:1000 for Western blots, 1:200 for immunostainings], eMHC (1:100 for Western blot, 1:1200 for immunostainings; developed by H. Blau, obtained from Developmental Studies Hybridoma Bank, catalog no. F1.652), F4/80 (1:100; Abcam, catalog no. ab6640), laminin-α1 (for detection of αLNNd by Western blot, 1:2000; R&D Systems, catalog no. AF4187), αLNNd [for detection of αLNNd by immunostainings, 1:100 (21)], laminin-α2 [for Western blot analysis (57), 1:500], laminin-α2 (N-terminal, for immunostainings of human samples, clone 4H8-2, 1:400; Sigma, catalog no. L0663), laminin-α2 (C-terminal, for immunostainings of human samples, clone 5H2, 1:5000; Merck Millipore, catalog no. MAB1922), laminin-α4 (21) (1:1000 for Western blots, 1:200 for immunostainings), laminin-α5 [clone 504, gift from L. Sorokin (58), 1:1000], laminin-β1γ1 (1:1000 for Western blots, 1:100 for immunostainings; Sigma, catalog no. L9393), laminin-

γ1 (1:200; Millipore, catalog no. MAB1914), Na^+/K^+-ATPase (1:1000; Cell Signaling, catalog no. 3010), GAPDH (1:1000; Cell Signaling, catalog no. 2118), and CD31 (1:100; Abcam, catalog no. ab9498).

Recombinant and native protein preparation for binding assays

Recombinant Lm-111, nidogen-1, and αLNNd were purified by hemagglutinin–affinity chromatography from stably transfected human embryonic kidney (HEK) 293 cells, as described (59). Mag was purified by metal-chelating chromatography, as described (20, 59, 60). Recombinant Lm-211 was purified by heparin affinity chromatography from cells grown in the presence 5 μM furin inhibitor-1 (Calbiochem, catalog no. 344930) to reduce LG domain cleavage (61). Recombinant Lm-511 containing Lmα5–C-terminal FLAG tag was purified from HEK293 by anti–FLAG-M2 affinity chromatography (60). Recombinant mouse nidogen-1 was purified from conditioned medium by HisPur-cobalt chelating chromatography (Thermo Scientific, catalog no. 89965). Type IV collagen was extracted and purified from lathyritic mouse EHS tumor, as described (62). Integrin constructs coding for soluble integrin α_7X_2 and integrin β_1 were stably transfected into 293 cells (J. Takagi, Osaka University, Japan) and purified on HisPur-cobalt chelating chromatography followed by FLAG-agarose affinity chromatography. αDG was extracted from rabbit muscles using wheat germ agglutinin–agarose beads (Vector Laboratories, catalog no. al-1023) as described (63) or as recombinant protein as described previously (64).

Polymerization assays

For polymerization assays, a 1:1 molar mixture of purified Lm-411 + αLNNd or Lm-411 and Lm-111 alone were incubated overnight on ice in 50 mM tris-HCl (pH 7.4), 90 mM NaCl, and 1 mM $CaCl_2$. Subsequently, aliquots of various concentrations were incubated at 37°C for 3 hours in polymerization buffer [50 mM tris-HCl (pH 7.4), 90 mM NaCl, 1 mM $CaCl_2$, 0.15% Triton X-100, bovine serum albumin (BSA) (30 ng/ml)]. Polymerized laminins were separated from nonpolymerized forms by centrifugation at 11,000g. Supernatant and pellet were loaded on SDS-PAGE followed by Coomassie blue staining and quantitation, as described (57, 60).

In vitro binding assays

To determine laminin binding to αDG, crude αDG was coated onto high-binding 96-well plates (Costar, catalog no. 3691) in bicarbonate buffer overnight at 4°C. Plates were incubated for 1 hour at room temperature with blocking buffer [50 mM tris-HCl (pH 7.4), 150 mM NaCl, 3% BSA, 1 mM $MgCl_2$,1 mM $CaCl_2$], washed with phosphate-buffered saline (PBS), and incubated with various amounts of recombinant laminins (in blocking buffer) for 2 hours at room temperature. Laminin binding was detected with aE4 (10 μg/ml; anti-Lm-111) antibodies and secondary anti-rabbit horseradish peroxidase (HRP), developed with Ultra-TMB (Thermo Scientific 34028), and absorbance was measured at 450 nm. To determine laminin binding to integrin $\alpha_7X_2\beta_1$, recombinant Lm-111 or Lm-411 (in bicarbonate buffer) was coated to high-binding 96-well plates overnight at 4°C. Plates were incubated for 1 hour at room temperature with blocking buffer [50 mM tris-HCl (pH 7.4), 90 mM NaCl, 1% BSA, 1 mM $MnCl_2$, 0.1% Tween-20], washed with PBS, and incubated with various concentrations of integrin $\alpha_7X_2\beta_1$ (in blocking buffer) for 2 hours at RT. Bound

integrin was detected with anti-VELCRO antibody (1:1000) and streptavidin-HRP antibodies and detected with Ultra-TMB, as described above.

Histology and histological quantifications

Muscles were mounted on 7% gum tragacanth (Sigma), and rapidly frozen 2-methylbutane was cooled in liquid nitrogen (-150°C). Cross sections of 12 μm thickness were cut on a cryostat. General histology was assessed after tissue fixation with 4% paraformaldehyde by H&E staining (Merck) or Picro Sirius Red stain [Direct Red 80 (Sigma) in picric acid solution]. Images were acquired with an Olympus iX81 microscope using cellSens software (Olympus). To assess the severity of muscular dystrophy, the H&E-stained cross sections were blindly examined and scored by two to three observers. The basis of the judgment was a qualitative extent of muscle degeneration, cell infiltration, fibrosis, the shape of muscle fibers and their number, size and size variation, and the number of fibers containing centralized myonuclei. Each mouse was given a relative value termed “dystrophic severity index” from 0 (no muscular dystrophy) to 4 (severe muscular dystrophy). For fiber number and fiber size analysis, laminin-γ1-stained mid-belly cross sections were evaluated using cellSens software (Olympus Soft Imaging System). The muscle fiber size was quantified using the minimum distance of parallel tangents at opposing particle borders (minimal “Feret’s diameter”), as described elsewhere (65). The fibrotic area in diaphragm was quantified as the percentage of Sirius Red-positive area per cross-sectional area.

Hydroxyproline assay

Fibrosis in muscles was determined by measuring the amount of collagen-specific amino acid hydroxyproline. Methods for isolation, freeze-drying, and amino acid analysis were as described (19). Amino acid analysis was done by the Analytical Research and Services, University of Bern, Bern, Switzerland.

Grip strength and in vitro muscle force measurement

Grip strength was assessed by placing the mice on a vertical grid and measuring its hang time. The experiment was stopped after 3 min. In vitro muscle force measurements were performed on isolated EDL and soleus muscle using the 1200A Isolated Muscle System (Aurora Scientific). By stimulation with a single electrical pulse (2.5 kHz, 15 V, 0.2 ms), muscles were adjusted to the optimum muscle length (L_o) achieved at peak twitch force (P_t). Peak tetanic force (P_o) was recorded with 500-ms stimulation (150 Hz for EDL, 120 Hz for soleus). Specific peak and twitch forces were calculated by normalization to the cross-sectional area (CSA) by using the following formula: CSA (mm^2) = muscle wet weight (mg)/[fiber length (l_f, mm) × 1.06 mg/mm^3], with $l_f = l_o \times 0.44$ for EDL or $l_f = l_o \times 0.71$ for soleus (66).

Statistical analysis

Statistical analysis was performed using unpaired, two-tailed Student’s *t* test for comparisons of two groups. Welch’s correction was applied if unequal variance between groups was detected by *F* test. One- or two-way ANOVA followed by Bonferroni post hoc test was used for the comparisons of more than two groups. We assumed normal distribution

of the variables analyzed. Survival analyses were performed using the Kaplan-Meier method, and the significance of differences between curves was calculated using the log-rank test. All statistical tests were performed using Prism version 6 (GraphPad Software). Statistical significance was set at $P < 0.05$. All data are presented as means ± SEM, unless indicated otherwise in the figure legend. Individual-level data and exact P values are shown in table S3.

Supplementary Material

Refer to Web version on PubMed Central for supplementary material.

Acknowledgments

We thank F. Oliveri for technical assistance throughout the project, U. Sauder for help in electron microscopy, P. Jenö for mass spectrometry, the animal facility for mouse handling, and the Transgenic Mouse Core facility of the University of Basel for cDNA injections into mouse embryos. We thank D. Ham for critical reading of the manuscript and N. Rion for sharing material. Neurotrypsin knockout mice were received from Neurotune Ltd. and C. Wagner (University of Zurich, Switzerland), and laminin-α5 antibodies were from L. Sorokin (University of Münster, Germany). We thank S. Frank (University Hospital Basel), S. Krause (Friedrich Baur Institute, Munich, Germany), M. Mora (C. Besta Neurological Institute, Milano, Italy), and M. Chapart (Hôpital de la Pitié-Salpêtrière, Paris, France) for providing biopsies.

Funding: This work was supported by the Cantons of Basel-Stadt and Basel-Landschaft, grants from the Swiss Foundation for Research on Muscle Diseases, the Association Française contre les Myopathies, and the Neuromuscular Research Association Basel.

REFERENCES AND NOTES

1. Mercuri E, Muntoni F. Muscular dystrophies. Lancet. 2013; 381:845–860. [PubMed: 23465426]
2. Norwood FLM, Harling C, Chinnery PF, Eagle M, Bushby K, Straub V. Prevalence of genetic muscle disease in Northern England: In-depth analysis of a muscle clinic population. Brain. 2009; 132:3175–3186. [PubMed: 19767415]
3. Clement EM, Feng L, Mein R, Sewry CA, Robb SA, Manzur AY, Mercuri E, Godfrey C, Cullup T, Abbs S, Muntoni F. Relative frequency of congenital muscular dystrophy subtypes: Analysis of the UK diagnostic service 2001–2008. Neuromuscul. Disord. 2012; 22:522–527. [PubMed: 22480491]
4. Geranmayeh F, Clement E, Feng LH, Sewry C, Pagan J, Mein R, Abbs S, Brueton L, Childs A-M, Jungbluth H, De Goede CG, Lynch B, Lin J-P, Chow G, Sousa C, O'Mahony O, Majumdar A, Straub V, Bushby K, Muntoni F. Genotype-phenotype correlation in a large population of muscular dystrophy patients with *LAMA2* mutations. Neuromuscul. Disord. 2010; 20:241–250. [PubMed: 20207543]
5. Guo LT, Zhang XU, Kuang W, Xu H, Liu LA, Vilquin J-T, Miyagoe-Suzuki Y, Takeda S, Ruegg MA, Wewer UM, Engvall E. Laminin α2 deficiency and muscular dystrophy; genotype-phenotype correlation in mutant mice. Neuromuscul. Disord. 2003; 13:207–215. [PubMed: 12609502]
6. Kuang W, Xu H, Vachon PH, Liu L, Loechel F, Wewer UM, Engvall E. Merosin-deficient congenital muscular dystrophy. Partial genetic correction in two mouse models. J. Clin. Invest. 1998; 102:844–852. [PubMed: 9710454]
7. Xu H, Wu X-R, Wewer UM, Engvall E. Murine muscular dystrophy caused by a mutation in the laminin α2 (*Lama2*) gene. Nat. Genet. 1994; 8:297–302. [PubMed: 7874173]
8. Colognato H, Yurchenco PD. The laminin α2 expressed by dystrophic dy^{2J} mice is defective in its ability to form polymers. Curr. Biol. 1999; 9:1327–1330. [PubMed: 10574769]
9. Patton BL, Miner JH, Chiu AY, Sanes JR. Distribution and function of laminins in the neuromuscular system of developing, adult, and mutant mice. J. Cell Biol. 1997; 139:1507–1521. [PubMed: 9396756]

10. Gullberg D, Tiger CF, Velling T. Laminins during muscle development and in muscular dystrophies. Cell. Mol. Life Sci. 1999; 56:442–460. [PubMed: 11212297]
11. Ringelmann B, Röder C, Hallmann R, Maley M, Davies M, Grounds M, Sorokin L. Expression of laminin α1 α2, α4 and α5 chains, fibronectin, and tenascin-C in skeletal muscle of dystrophic 129ReJ*dy/dy* mice. Exp. Cell Res. 1999; 246:165–182. [PubMed: 9882526]
12. Moll J, Barzaghi P, Lin S, Bezakova G, Lochmüller H, Engvall E, Müller U, Ruegg MA. An agrin minigene rescues dystrophic symptoms in a mouse model for congenital muscular dystrophy. Nature. 2001; 413:302–307. [PubMed: 11565031]
13. Li S, Harrison D, Carbonetto S, Fassler R, Smyth N, Edgar D, Yurchenco PD. Matrix assembly, regulation, and survival functions of laminin and its receptors in embryonic stem cell differentiation. J. Cell Biol. 2002; 157:1279–1290. [PubMed: 12082085]
14. Yurchenco PD. Basement membranes: Cell scaffoldings and signaling platforms. Cold Spring Harb. Perspect. Biol. 2011; 3:a004911. [PubMed: 21421915]
15. Talts JF, Sasaki T, Miosge N, Göhring W, Mann K, Mayne R, Timpl R. Structural and functional analysis of the recombinant G domain of the laminin α4 chain and its proteolytic processing in tissues. J. Biol. Chem. 2000; 275:35192–35199. [PubMed: 10934193]
16. von der Mark H, Williams I, Wendler O, Sorokin L, von der Mark K, Pöschl E. Alternative splice variants of $\alpha_7\beta_1$ integrin selectively recognize different laminin isoforms. J. Biol. Chem. 2002; 277:6012–6016. [PubMed: 11744715]
17. Nishiuchi R, Takagi J, Hayashi M, Ido H, Yagi Y, Sanzen N, Tsuji T, Yamada M, Sekiguchi K. Ligand-binding specificities of laminin-binding integrins: A comprehensive survey of laminin–integrin interactions using recombinant α3β1, α6β1, α7β1 and α6β4 integrins. Matrix Biol. 2006; 25:189–197. [PubMed: 16413178]
18. Bentzinger CF, Barzaghi P, Lin S, Ruegg MA. Overexpression of mini-agrin in skeletal muscle increases muscle integrity and regenerative capacity in laminin-α2-deficient mice. FASEB J. 2005; 19:934–942. [PubMed: 15923403]
19. Meinen S, Barzaghi P, Lin S, Lochmüller H, Ruegg MA. Linker molecules between laminins and dystroglycan ameliorate laminin-α2-deficient muscular dystrophy at all disease stages. J. Cell Biol. 2007; 176:979–993. [PubMed: 17389231]
20. McKee KK, Capizzi S, Yurchenco PD. Scaffold-forming and adhesive contributions of synthetic laminin-binding proteins to basement membrane assembly. J. Biol. Chem. 2009; 284:8984–8994. [PubMed: 19189961]
21. McKee KK, Crosson SC, Meinen S, Reinhard JR, Ruegg MA, Yurchenco PD. Chimeric protein repair of laminin polymerization ameliorates muscular dystrophy phenotype. J. Clin. Invest. 2017; 127:1075–1089. [PubMed: 28218617]
22. Patton BL, Connolly AM, Martin PT, Cunningham JM, Mehta S, Pestronk A, Miner JH, Sanes JR. Distribution of ten laminin chains in dystrophic and regenerating muscles. Neuromuscul. Disord. 1999; 9:423–433. [PubMed: 10545049]
23. Sewry CA, Philpot J, Mahony D, Wilson LA, Muntoni F, Dubowitz V. Expression of laminin subunits in congenital muscular dystrophy. Neuromuscul. Disord. 1995; 5:307–316. [PubMed: 7580244]
24. Yurchenco PD, Patton BL. Developmental and pathogenic mechanisms of basement membrane assembly. Curr. Pharm. Des. 2009; 15:1277–1294. [PubMed: 19355968]
25. Denzer AJ, Brandenberger R, Gesemann M, Chiquet M, Ruegg MA. Agrin binds to the nerve-muscle basal lamina via laminin. J. Cell Biol. 1997; 137:671–683. [PubMed: 9151673]
26. Kammerer RA, Schulthess T, Landwehr R, Schumacher B, Lustig A, Yurchenco PD, Ruegg MA, Engel J, Denzer AJ. Interaction of agrin with laminin requires a coiled-coil conformation of the agrin-binding site within the laminin γ1 chain. EMBO J. 1999; 18:6762–6770. [PubMed: 10581249]
27. Gesemann M, Cavalli V, Denzer AJ, Brancaccio A, Schumacher B, Ruegg MA. Alternative splicing of agrin alters its binding to heparin, dystroglycan, and the putative agrin receptor. Neuron. 1996; 16:755–767. [PubMed: 8607994]
28. Martin PT, Sanes JR. Integrins mediate adhesion to agrin and modulate agrin signaling. Development. 1997; 124:3909–3917. [PubMed: 9367446]

29. Meinen S, Lin S, Thurnherr R, Erb M, Meier T, Rüegg MA. Apoptosis inhibitors and mini-agrin have additive benefits in congenital muscular dystrophy mice. EMBO Mol. Med. 2011; 3:465–479. [PubMed: 21674808]
30. Reif R, Sales S, Hettwer S, Dreier B, Gisler C, Wölfel J, Lüscher D, Zurlinden A, Stephan A, Ahmed S, Baici A, Ledermann B, Kunz B, Sonderegger P. Specific cleavage of agrin by neurotrypsin, a synaptic protease linked to mental retardation. FASEB J. 2007; 21:3468–3478. [PubMed: 17586728]
31. Doe JA, Wuebbles RD, Allred ET, Rooney JE, Elorza M, Burkin DJ. Transgenic overexpression of the α7 integrin reduces muscle pathology and improves viability in the dy^W mouse model of merosin-deficient congenital muscular dystrophy type 1A. J. Cell Sci. 2011; 124:2287–2297. [PubMed: 21652631]
32. Mehuron T, Kumar A, Duarte L, Yamauchi J, Accorsi A, Girgenrath M. Dysregulation of matricellular proteins is an early signature of pathology in laminin-deficient muscular dystrophy. Skelet. Muscle. 2014; 4:14. [PubMed: 25075272]
33. Kuang W, Xu H, Vilquin JT, Engvall E. Activation of the lama2 gene in muscle regeneration: Abortive regeneration in laminin alpha2-deficiency. Lab. Invest. 1999; 79:1601–1613. [PubMed: 10616210]
34. Yamauchi J, Kumar A, Duarte L, Mehuron T, Girgenrath M. Triggering regeneration and tackling apoptosis: A combinatorial approach to treating congenital muscular dystrophy type 1 A. Hum. Mol. Genet. 2013; 22:4306–4317. [PubMed: 23773998]
35. Gawlik KI, Durbeej M. Skeletal muscle laminin and MDC1A: Pathogenesis and treatment strategies. Skelet. Muscle. 2011; 1:9. [PubMed: 21798088]
36. Huijbregts J, White JD, Grounds MD. The absence of MyoD in regenerating skeletal muscle affects the expression pattern of basement membrane, interstitial matrix and integrin molecules that is consistent with delayed myotube formation. Acta Histochem. 2001; 103:379–396. [PubMed: 11700944]
37. Tiger C-F, Champliaud M-F, Pedrosa-Domellof F, Thornell L-E, Ekblom P, Gullberg D. Presence of laminin α5 chain and lack of laminin α1 chain during human muscle development and in muscular dystrophies. J. Biol. Chem. 1997; 272:28590–28595. [PubMed: 9353324]
38. Funk SD, Miner JH. Muscular dystrophy meets protein biochemistry, the mother of invention. J. Clin. Invest. 2017; 127:798–800. [PubMed: 28218619]
39. Engvall E, Wewer UM. The new frontier in muscular dystrophy research: Booster genes. FASEB J. 2003; 17:1579–1584. [PubMed: 12958164]
40. Habashi JP, Judge DP, Holm TM, Cohn RD, Loeys BL, Cooper TK, Myers L, Klein EC, Liu G, Calvi C, Podowski M, Neptune ER, Halushka MK, Bedja D, Gabrielson K, Rifkin DB, Carta L, Ramirez F, Huso DL, Dietz HC. Losartan, an AT1 antagonist prevents aortic aneurysm in a mouse model of Marfan syndrome. Science. 2006; 312:117–121. [PubMed: 16601194]
41. Cohn RD, van Erp C, Habashi JP, Soleimani AA, Klein EC, Lisi MT, Gamradt M, ap Rhys CM, Holm TM, Loeys BL, Ramirez F, Judge DP, Ward CW, Dietz HC. Angiotensin II type 1 receptor blockade attenuates TGF-β-induced failure of muscle regeneration in multiple myopathic states. Nat. Med. 2007; 13:204–210. [PubMed: 17237794]
42. Elbaz M, Yanay N, Aga-Mizrachi S, Brunschwig Z, Kassis I, Ettinger K, Barak V, Nevo Y. Losartan, a therapeutic candidate in congenital muscular dystrophy: Studies in the dy^{2J}/dy^{2J} mouse. Ann. Neurol. 2012; 71:699–708. [PubMed: 22522482]
43. Bornstein P, Sage EH. Matricellular proteins: Extracellular modulators of cell function. Curr. Opin. Cell Biol. 2002; 14:608–616. [PubMed: 12231357]
44. Accorsi A, Kumar A, Rhee Y, Miller A, Girgenrath M. IGF-1/GH axis enhances losartan treatment in Lama2-related muscular dystrophy. Hum. Mol. Genet. 2016; 25:4624–4634. [PubMed: 27798092]
45. Gawlik K, Miyagoe-Suzuki Y, Ekblom P, Takeda S, Durbeej M. Laminin α1 chain reduces muscular dystrophy in laminin α2 chain deficient mice. Hum. Mol. Genet. 2004; 13:1775–1784. [PubMed: 15213105]

46. Gawlik KI, Durbeej M. Transgenic overexpression of laminin α1 chain in laminin α2 chain-deficient mice rescues the disease throughout the lifespan. Muscle Nerve. 2010; 42:30–37. [PubMed: 20544910]
47. Van Ry PM, Minogue P, Hodges BL, Burkin DJ. Laminin-111 improves muscle repair in a mouse model of merosin-deficient congenital muscular dystrophy. Hum. Mol. Genet. 2014; 23:383–396. [PubMed: 24009313]
48. Rooney JE, Knapp JR, Hodges BL, Wuebbles RD, Burkin DJ. Laminin-111 protein therapy reduces muscle pathology and improves viability of a mouse model of merosin-deficient congenital muscular dystrophy. Am. J. Pathol. 2012; 180:1593–1602. [PubMed: 22322301]
49. Qiao C, Li J, Zhu T, Draviam R, Watkins S, Ye X, Chen C, Xiao X. Amelioration of laminin-α2-deficient congenital muscular dystrophy by somatic gene transfer of miniagrin. Proc. Natl. Acad. Sci. U.S.A. 2005; 102:11999–12004. [PubMed: 16103356]
50. Buchlis G, Podsakoff GM, Radu A, Hawk SM, Flake AW, Mingozzi F, High KA. Factor IX expression in skeletal muscle of a severe hemophilia B patient 10 years after AAV-mediated gene transfer. Blood. 2012; 119:3038–3041. [PubMed: 22271447]
51. Mendell JR, Campbell K, Rodino-Klapac L, Sahenk Z, Shilling C, Lewis S, Bowles D, Gray S, Li C, Galloway G, Malik V, Coley B, Clark KR, Li J, Xiao X, Samulski J, McPhee SW, Samulski RJ, Walker CM. Dystrophin immunity in Duchenne's muscula dystrophy. N. Engl. J. Med. 2010; 363:1429–1437. [PubMed: 20925545]
52. Mack DL, Poulard K, Goddard MA, Latournerie V, Snyder JM, Grange RW, Elverman MR, Denard J, Veron P, Buscara L, Le Bec C, Hogrel J-Y, Brezovec AG, Meng H, Yang L, Liu F, O'Callaghan M, Gopal N, Kelly VE, Smith BK, Strande JL, Mavilio F, Beggs AH, Mingozzi F, Lawlor MW, Buj-Bello A, Childers MK. Systemic AAV8-mediated gene therapy drives whole-body correction of myotubular myopathy in dogs. Mol. Ther. 2017; 25:839–854. [PubMed: 28237839]
53. Turturro A, Duffy P, Hass B, Kodell R, Hart R. Survival characteristics and age-adjusted disease incidences in C57BL/6 mice fed a commonly used cereal-based diet modulated b dietary restriction. J. Gerontol. A Biol. Sci. Med. Sci. 2002; 57:B379–B389. [PubMed: 12403793]
54. Bonnemann CG, Wang CH, Quijano-Roy S, Deconinck N, Bertini E, Ferreiro A, Muntoni F, Sewry C, Beroud C, Mathews KD, Moore SA, Bellini J, Rutkowski A, North KN. Diagnostic approach to the congenital muscular dystrophies. Neuromuscul. Disord. 2014; 24:289–311. [PubMed: 24581957]
55. Chan SHS, Foley AR, Phadke R, Mathew AA, Pitt M, Sewry C, Muntoni F. Limb girdle muscular dystrophy due to *LAMA2* mutations: Diagnostic difficulties due to associated peripheral neuropathy. Neuromuscul. Disord. 2014; 24:677–683. [PubMed: 24957499]
56. Gesemann M, Denzer AJ, Ruegg MA. Acetylcholine receptor-aggregating activity of agrin isoforms and mapping of the active site. J. Cell Biol. 1995; 128:625–636. [PubMed: 7860635]
57. Cheng Y-S, Champliaud M-F, Burgeson RE, Marinkovich MP, Yurchenco PD. Self-assembly of laminin isoforms. J. Biol. Chem. 1997; 272:31525–31532. [PubMed: 9395489]
58. Song J, Lokmic Z, Lämmermann T, Rolf J, Wu C, Zhang X, Hallmann R, Hannocks M-J, Horn N, Ruegg MA, Sonnenberg A, Georges-Labouesse E, Winkler TH, Kearney JF, Cardell S, Sorokin L. Extracellular matrix of secondary lymphoid organs impacts on B-cell fate and survival. Proc. Natl. Acad. Sci. U.S.A. 2013; 110:E2915–E2924. [PubMed: 23847204]
59. McKee KK, Yang D-H, Patel R, Chen Z-L, Strickland S, Takagi J, Sekiguchi K, Yurchenco PD. Schwann cell myelination requires integration of laminin activities. J. Cel Sci. 2012; 125:4609–4619.
60. McKee KK, Harrison D, Capizzi S, Yurchenco PD. Role of laminin terminal globular domains in basement membrane assembly. J. Biol. Chem. 2007; 282:21437–21447. [PubMed: 17517882]
61. Smirnov SP, Barzaghi P, McKee KK, Ruegg MA, Yurchenco PD. Conjugation of LG domains of agrins and perlecan to polymerizing laminin-2 promotes acetylcholine receptor clustering. J. Biol. Chem. 2005; 280:41449–41457. [PubMed: 16219760]
62. Yurchenco PD, Furthmayr H. Self-assembly of basement membrane collagen. Biochemistry. 1984; 23:1839–1850. [PubMed: 6722126]

63. Michele DE, Barresi R, Kanagawa M, Saito F, Cohn RD, Satz JS, Dollar J, Nishino I, Kelley RI, Somer H, Straub V, Mathews KD, Moore SA, Campbell KP. Post-translational disruption of dystroglycan-ligand interactions in congenital muscular dystrophies. Nature. 2002; 418:417–422. [PubMed: 12140558]

64. Yoon JH, Xu R, Martin P. A method to produce and purify full-length recombinant alpha dystroglycan: Analysis of N- and O-linked monosaccharide composition in CHO cells with or without LARGE overexpression. PLOS Curr. 2013; 5

65. Briguet A, Courdier-Fruh I, Foster M, Meier T, Magyar JP. Histological parameters for the quantitative assessment of muscular dystrophy in the mdx-mouse. Neuromuscul. Disord. 2004; 14:675–682. [PubMed: 15351425]

66. Brooks SV, Faulkner JA. Contractile properties of skeletal muscles from young, adult and aged mice. J. Physiol. 1988; 404:71–82. [PubMed: 3253447]

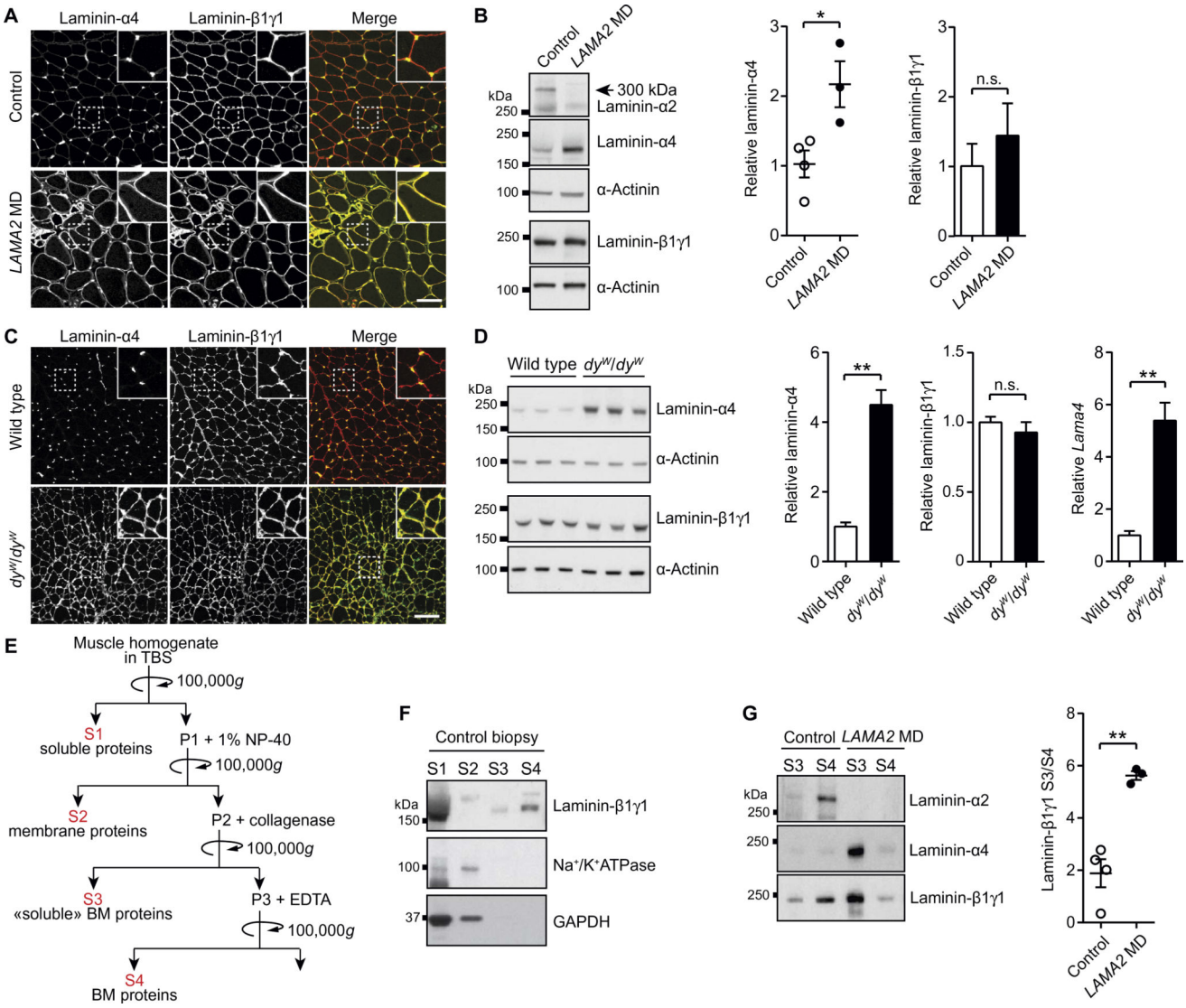

Fig. 1. Muscles of *LAMA2* MD patients and dy^W/dy^W mice contain high amounts of laminin-α4 and show deficits in BM

(**A**) Representative immunofluorescence images (magnified images in insets) of human muscle biopsy cross sections stained for laminin-α4 and laminin-β1γ1. $n = 3$ *LAMA2* MD patients or healthy controls. (**B**) Western blot analysis and quantification of laminin chains in human muscle biopsies. α-Actinin was used as loading control. $n = 4$ controls, $n = 3$ *LAMA2* MD patients. (**C**) Representative immunofluorescence images (magnified images in insets) of triceps muscle from 8-week-old mice stained for laminin-α4 and laminin-β1γ1. $n = 4$ mice per genotype. (**D**) Western blot analysis and quantification of laminin-α4 (left graph), laminin-β1γ1 (middle graph), and *Lama4* transcripts (right graph) from triceps muscle of 8-week-old mice. $n = 3$ mice per genotype (Western blot) and $n = 4$ mice per genotype (quantitative reverse transcription polymerase chain reaction). (**E**) Schematic of subcellular fractionation. (**F**) Western blot analysis of S1 to S4 of a muscle biopsy from a control patient. Glyceraldehyde-3-phosphate dehydrogenase (GAPDH) and Na^+/K^+-ATPase (sodium-potassium adenosine triphosphatase) were used as markers for cytosolic and

membrane proteins, respectively. (**G**) Western blot analysis of S3 and S4 fractions from control and *LAMA2* MD patient muscle biopsies probed for the indicated proteins. Right: Ratio of the laminin-β1γ1 intensity in S3 and S4 fraction. $n = 4$ healthy controls, $n = 3$ *LAMA2* MD patients. Data are means ± SEM. *$P < 0.05$; **$P < 0.01$; n.s. (not significant), $P > 0.05$ (for exact P values, see table S3), Student's t test. Scale bars, 100 μm (A and C).

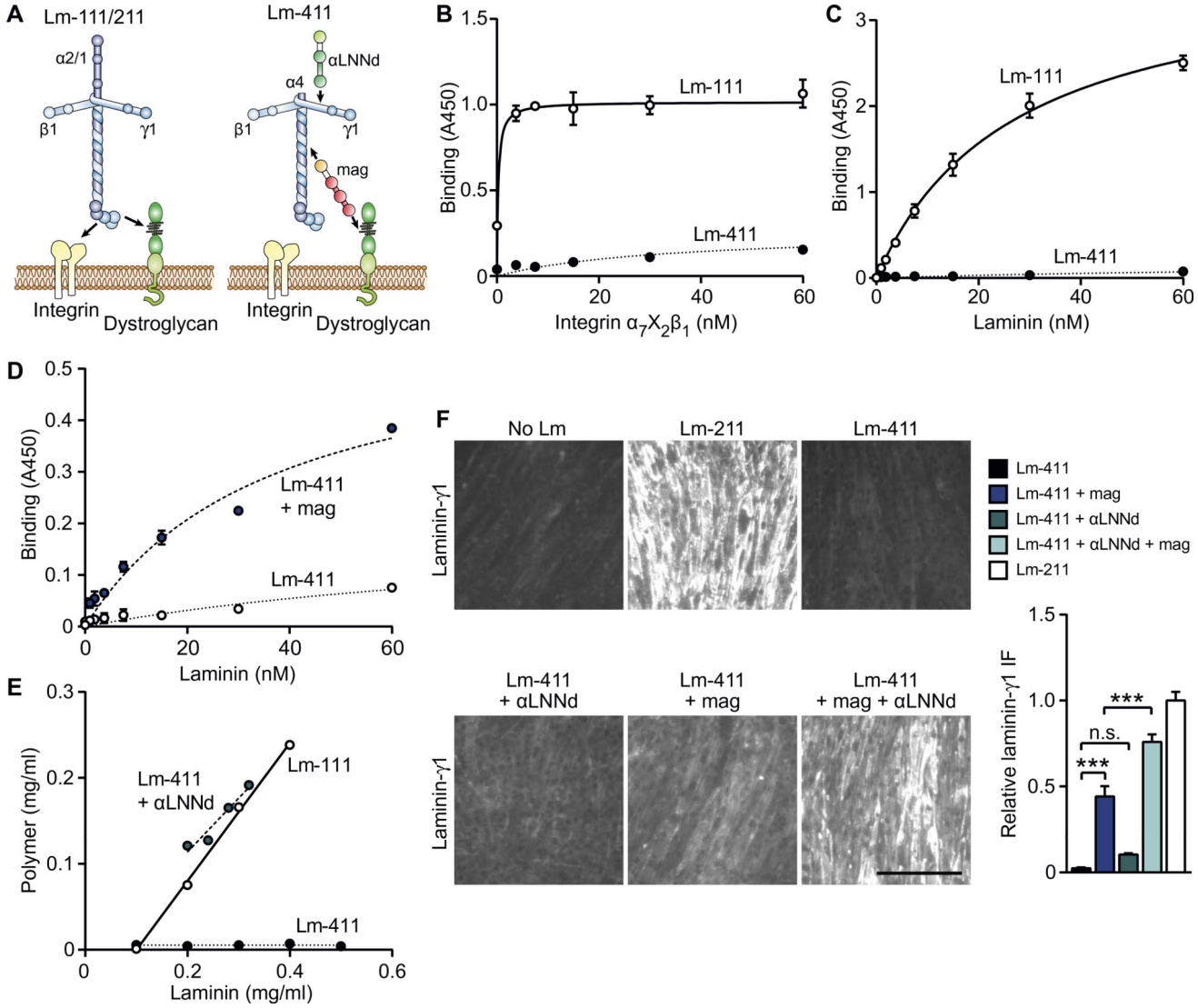

Fig. 2. Binding of recombinant full-length Lm-411 to muscle receptors, myotubes, and self-polymerization is enhanced by mag and αLNNd

(**A**) Schematic of Lm-111, Lm-211, and Lm-411 and the linker molecules mag and αLNNd. Binding interactions of mag, αLNNd, laminins, integrins, and dystroglycan are indicated. (**B**) Binding curves of integrin $\alpha_7X_2\beta_1$ to Lm-111 and Lm-411. (**C**) Binding curves of Lm-111 and Lm-411 to purified αDG. (**D**) Binding curves of Lm-411 and Lm-411 plus an equimolar concentration of mag to purified αDG. Data in (B) to (D) are means ± SEM with $n = 3$ per condition. Curve fitting used the equation $Y = B_{max}*X/(K_d + X)$. (**E**) Polymerization assay for Lm-111, Lm-411, and an equimolar mixture of Lm-411 and αLNNd. Polymer formation was monitored by SDS–polyacrylamide gel electrophoresis (PAGE) and Coomassie blue staining after centrifugation. $r^2 = 0.998$ (Lm-111), $r^2 = 0.941$ (Lm-411 and αLNNd), and $r^2 = 0.0013$ (Lm-411) using linear regression. (**F**) Confluent layer of cultured C2C12 myotubes after incubation with no Lm, recombinant Lm-211, Lm-411, or Lm-411 in the presence of an equimolar concentration of αLNNd and/or mag. C2C12-bound Lm-211 or Lm-411 was visualized by staining with antibodies to laminin-γ1.

Representative immunofluorescence images (left) and quantification (right) of laminin-γ1 immunofluorescence (IF). Scale bar, 200 μm. $n = 9$ cultures (Lm-411 and mag), $n = 6$ cultures (Lm-411, Lm-411 + αLNNd, Lm-411 + αLNNd + mag, and Lm-211). Data are means ± SEM. ***$P < 0.001$; n.s., $P > 0.05$ (for exact P values, see table S3), one-way analysis of variance (ANOVA) with Bonferroni post hoc test.

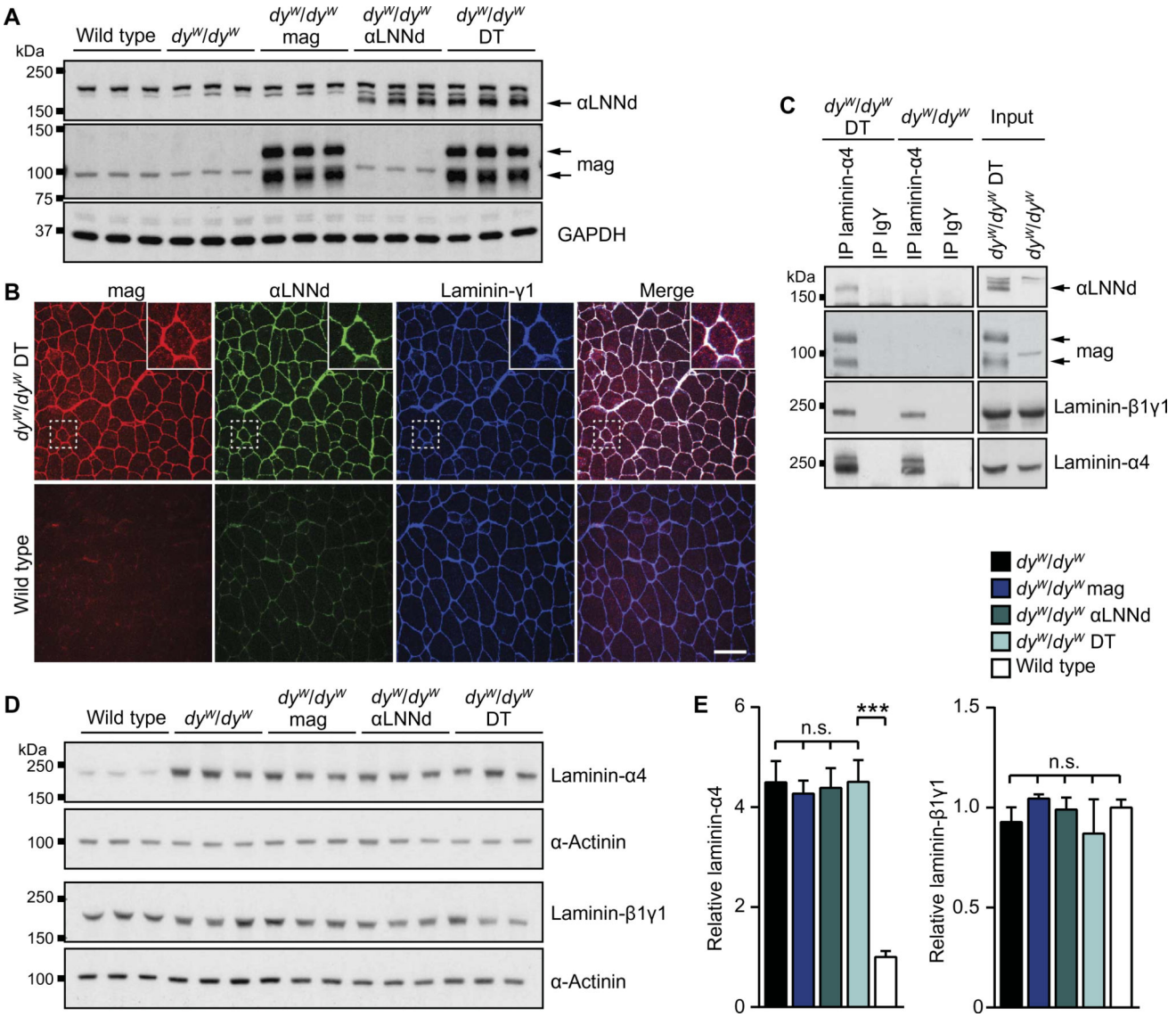

Fig. 3. Transgenic expression of mag and αLNNd in dy^W/dy^W mice

(**A**) Western blot analysis to detect αLNNd and mag in lysates from triceps muscle from 8-week-old mice. GAPDH was used as loading control. The αLNNd-specific band is indicated by an arrow because the antibodies also detect nonspecific bands at higher M_r; mag runs on SDS-PAGE as two bands because of its cleavage by neurotrypsin (see fig. S5, F and G, for details). (**B**) Representative immunofluorescence (magnified images in insets) images of triceps cross sections from 8-week-old mice stained for mag, αLNNd, and laminin-γ1. $n = 4$ mice per genotype. Scale bar, 100 μm. (**C**) Western blot analysis of immunoprecipitates using anti–laminin-α4 antibodies or immunoglobulin Y (IgY) (as control) and lysates of triceps muscle from 8-week-old dy^W/dy^W DT or dy^W/dy^W mice. (**D**) Western blot analysis of laminin-α4 and laminin-β1γ1 in lysates of triceps muscles from 8-week-old mice. α-Actinin was used as loading control. (**E**) Protein quantification in lysates from the different mice. $n = 3$ mice per genotype. Data are means ± SEM. ***$P < 0.001$; n.s., $P > 0.05$ (for exact P values, see table S3), one-way ANOVA with Bonferroni post hoc test.

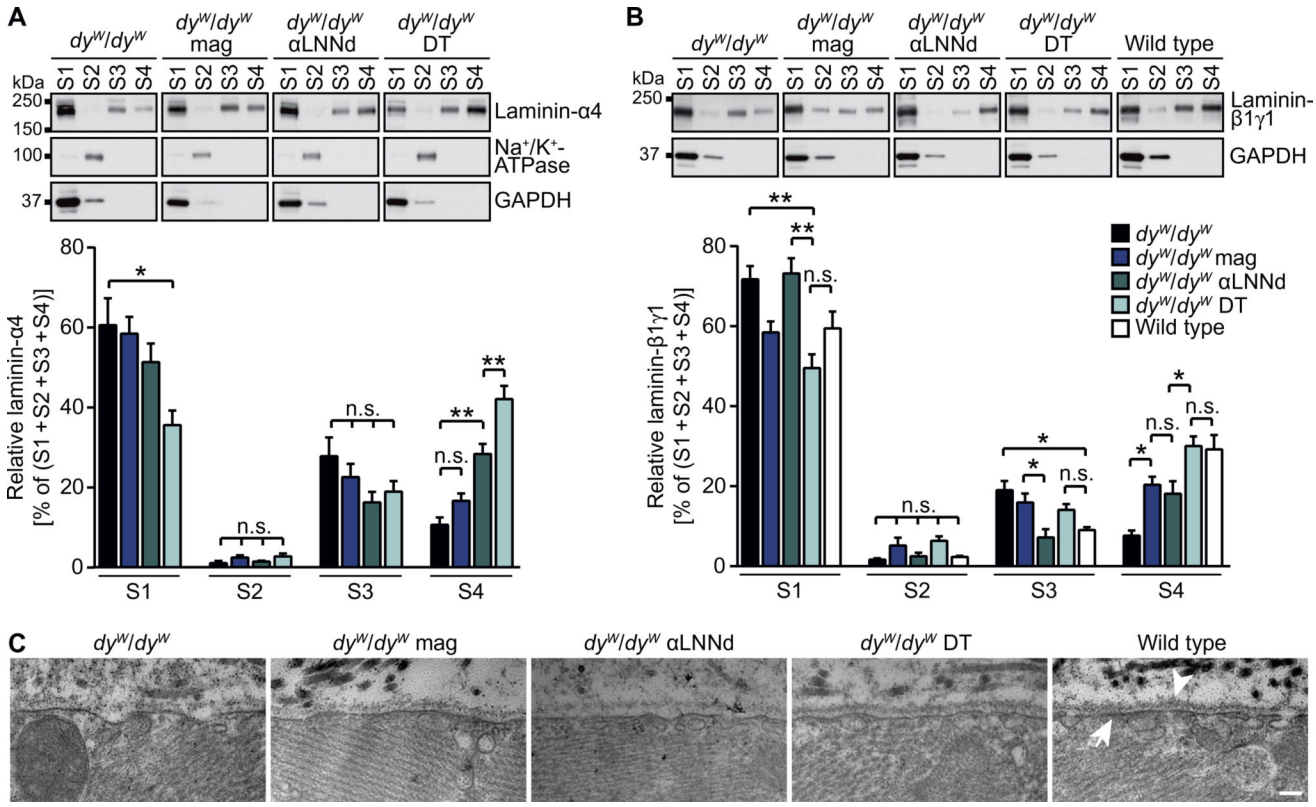

Fig. 4. Expression of mag and αLNNd in dy^W/dy^W mice improves muscle BM

(**A** and **B**) Western blot analysis (top) and quantification (bottom) of laminin-α4 (A) and laminin-β1γ1 (B) in the fractions obtained by differential extraction of triceps muscles of 8-week-old mice (see scheme in Fig. 1E). GAPDH and Na^+/K^+-ATPase were used as markers for the soluble (S1) and the membrane proteins (S2), respectively. $n = 4$ mice (dy^W/dy^W), $n = 6$ mice (dy^W/dy^W mag, dy^W/dy^W αLNNd, and dy^W/dy^W DT), $n = 5$ mice (wild type). Data are means ± SEM. $^*P < 0.05$; $^{**}P < 0.01$; n.s., $P > 0.05$ (for exact P values, see table S3), one-way ANOVA with Bonferroni post hoc test. (**C**) Transmission electron micrographs of triceps muscle from 8-week-old mice. White arrow, sarcolemma; white arrowhead, BM. Scale bar, 100 nm.

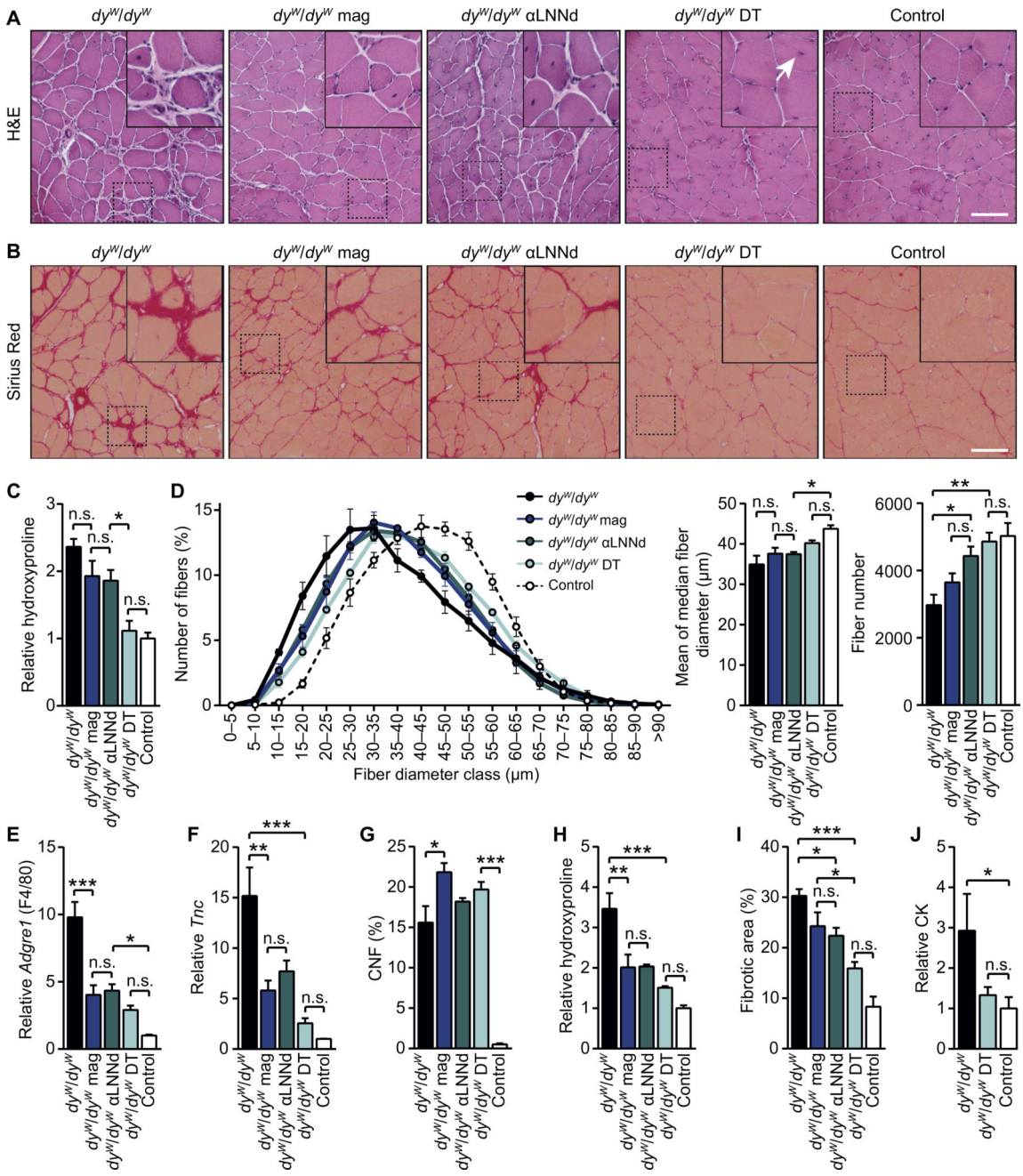

Fig. 5. Transgenic expression of α LNNd and mag in dy^W/dy^W mice improves muscle histology in 8-week-old mice

(**A**) Representative images (magnified images in insets) of H&E-stained cross sections from triceps muscle. An example of a muscle fiber with centralized myonuclei is indicated with an arrow. *n* = 5 mice per genotype. (**B**) Representative images (magnified images in insets) of Sirius Red–stained cross sections (collagen in red) from triceps muscle. *n* = 3 mice per genotype. (**C**) Relative hydroxyproline content in triceps indicative of collagen content. Values are normalized to controls. *n* =4 mice (dy^W/dy^W mag, dy^W/dy^W αLNNd, and dy^W/dy^W DT), *n* = 5 mice (dy^W/dy^W), *n* = 6 mice (control). (**D**) Distribution of the muscle

fiber diameters (left), the mean of median fiber diameter (middle), and the total fiber number (right) in 8-week-old triceps muscle. $n = 4$ male mice (dy^W/dy^W and control), $n = 5$ male mice (dy^W/dy^W αLNNd and dy^W/dy^W DT), $n = 6$ male mice (dy^W/dy^W mag). Statistical evaluation of fiber size distribution is shown in table S1. (**E**) Expression of the inflammatory marker *Adgre1* (encoding F4/80). $n = 4$ mice (dy^W/dy^W, dy^W/dy^W mag, dy^W/dy^W αLNNd, and control), $n = 5$ mice (dy^W/dy^W DT). (**F**) Expression of transcripts encoding the matricellular protein tenascin-C in triceps muscle. $n = 4$ mice (dy^W/dy^W mag, dy^W/dy^W αLNNd, and control), $n = 5$ mice (dy^W/dy^W and dy^W/dy^W DT). (**G**) Quantification of CNFs in triceps muscle. $n = 3$ mice per genotype. (**H**) Quantification of relative hydroxyproline content in TA from 8-week-old mice. $n = 3$ mice (dy^W/dy^W DT), $n = 4$ mice (dy^W/dy^W mag and dy^W/dy^W αLNNd), $n = 5$ mice (dy^W/dy^W), $n = 6$ mice (control). (**I**) Quantification of fibrotic area (visualized by Sirius Red staining) in diaphragm cross sections. $n = 4$ mice (dy^W/dy^W and dy^W/dy^W mag), $n = 7$ mice (dy^W/dy^W αLNNd, dy^W/dy^W DT, and control). (**J**) Creatine kinase activity in blood. $n = 7$ mice (dy^W/dy^W and dy^W/dy^W DT), $n = 15$ mice (control). Data are means ± SEM. $*P < 0.05$; $**P < 0.01$; $***P < 0.001$; n.s., $P > 0.05$ (for exact P values, see table S3), one-way ANOVA with Bonferroni post hoc test. Controls are wild-type or $dy^W/+$ littermates. Scale bars, 100 μm.

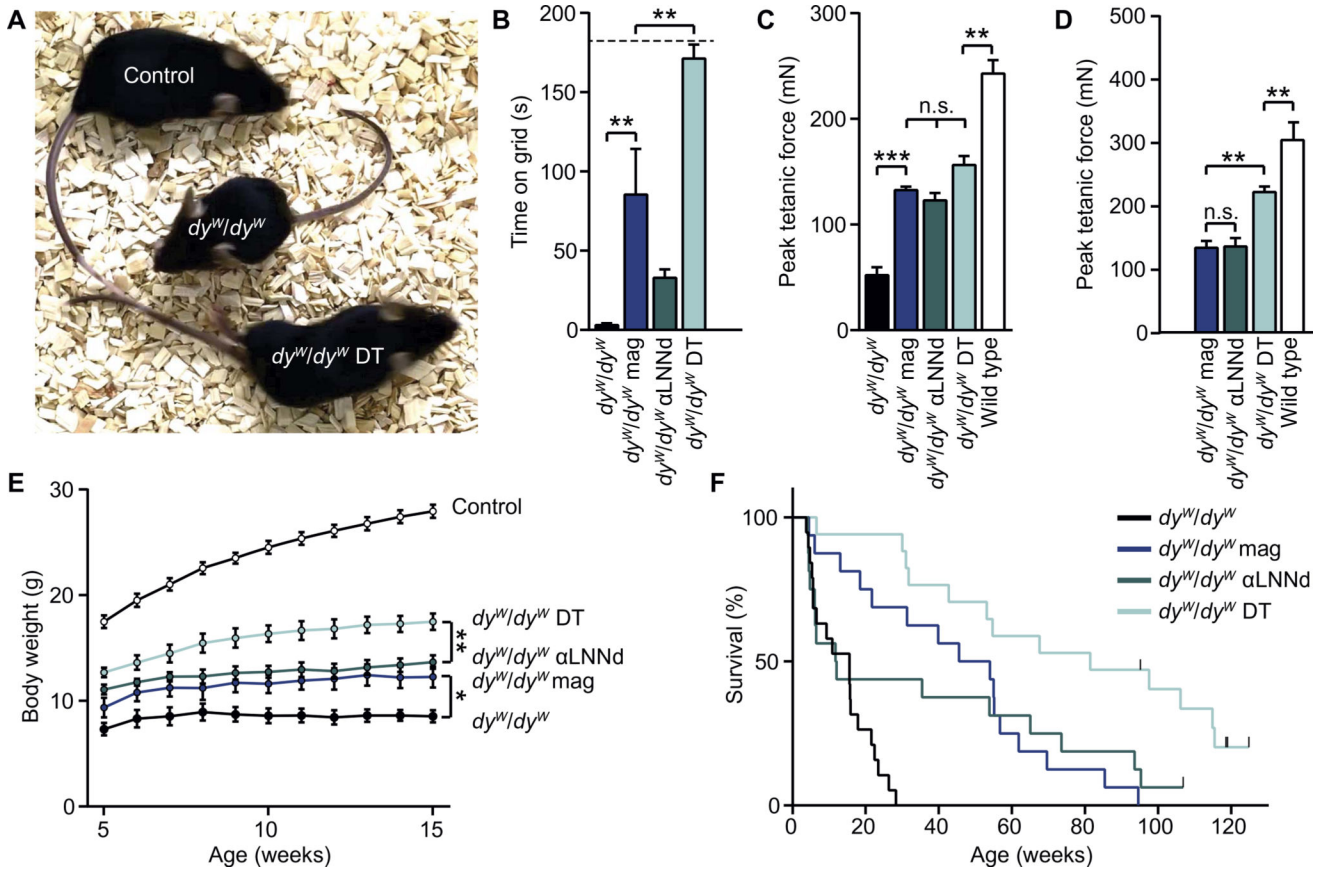

Fig. 6. Transgenic expression of αLNNd and mag in dy^W/dy^W mice improves muscle function, increases body weight, and prolongs life span

(**A**) Picture of a representative dy^W/dy^W, dy^W/dy^W DT, and control mouse (8 weeks old). Note that dy^W/dy^W mice appear small because of the severe kyphosis, and dy^W/dy^W DT mice are leaner than controls. $n = 10$ mice per genotype. (**B**) Quantification of grip strength of 8-week-old mice. Grip strength was measured by hang time on a vertical grid. Test was stopped after 180 s (dotted line). $n = 4$ mice (dy^W/dy^W), $n = 6$ mice (dy^W/dy^W mag), $n = 7$ mice (dy^W/dy^W αLNNd), $n = 9$ mice (dy^W/dy^W DT). (**C**) Peak tetanic force of EDL muscle from 8-week-old mice. $n = 9$ mice (dy^W/dy^W), $n = 10$ mice (dy^W/dy^W mag), $n = 12$ mice (dy^W/dy^W αLNNd), $n = 13$ mice (dy^W/dy^W DT), $n = 14$ mice (control). (**D**) Peak tetanic force of EDL from 16-week-old mice. $n = 4$ mice (dy^W/dy^W αLNNd), $n = 5$ mice (dy^W/dy^W mag and control), $n = 6$ mice (dy^W/dy^W DT). Data in (B) and (C) are means ± SEM. $^*P < 0.05$; $^{**}P < 0.01$; $^{***}P < 0.001$; n.s., $P > 0.05$ (for exact P values, see table S3), one-way ANOVA with Bonferroni post hoc test. (**E**) Body weight of 5- to 15-week-old male mice. Mice that died between 5 and 15 weeks of age were excluded from analysis. $n = 7$ mice (dy^W/dy^W), $n = 6$ (dy^W/dy^W mag and dy^W/dy^W αLNNd), $n = 11$ mice (dy^W/dy^W DT), $n = 8$ mice (control). Data are means ± SEM. $^*P < 0.05$, $^{**}P < 0.01$ (for exact P values, see table S3), two-way ANOVA with Bonferroni post hoc test. (**F**) Survival curves for dy^W/dy^W ($n = 19$), dy^W/dy^W mag ($n = 16$), dy^W/dy^W αLNNd ($n = 16$), and dy^W/dy^W DT ($n = 17$) mice. Marks indicate mice that were still alive at the end of the study. $^{**}P < 0.01$ (dy^W/dy^W mag versus dy^W/dy^W DT), $^{***}P < 0.001$ (dy^W/dy^W versus dy^W/dy^W DT or dy^W/dy^W versus

dy^{W}/dy^{W} mag) (for exact *P* values, see table S3), log-rank test. Controls are wild-type or $dy^{W}/+$ littermates.